Microenvironment and Immunology

Cancer Research

Stress Signaling from Human Mammary Epithelial Cells Contributes to Phenotypes of Mammographic Density

Rosa Anna DeFilippis[1,2], Colleen Fordyce[1,2], Kelley Patten[1,2], Hang Chang[3], Jianxin Zhao[1,2], Gerald V. Fontenay[3], Karla Kerlikowske[4,5,6], Bahram Parvin[3,7], and Thea D. Tlsty[1,2]

Abstract

Telomere malfunction and other types of DNA damage induce an activin A–dependent stress response in mortal nontumorigenic human mammary epithelial cells that subsequently induces desmoplastic-like phenotypes in neighboring fibroblasts. Some characteristics of this fibroblast/stromal response, such as reduced adipocytes and increased extracellular matrix content, are observed not only in tumor tissues but also in disease-free breast tissues at high risk for developing cancer, especially high mammographic density tissues. We found that these phenotypes are induced by repression of the fatty acid translocase CD36, which is seen in desmoplastic and disease-free high mammographic density tissues. In this study, we show that epithelial cells from high mammographic density tissues have more DNA damage signaling, shorter telomeres, increased activin A secretion and an altered DNA damage response compared with epithelial cells from low mammographic density tissues. Strikingly, both telomere malfunction and activin A expression in epithelial cells can repress *CD36* expression in adjacent fibroblasts. These results provide new insights into how high mammographic density arises and why it is associated with breast cancer risk, with implications for the definition of novel invention targets (e.g., activin A and CD36) to prevent breast cancer. *Cancer Res; 74(18); 5032–44. ©2014 AACR.*

Introduction

Histologic examination demonstrates that tumor stroma is morphologically distinct from disease-free stroma. It is characterized by increases in extracellular matrix (ECM), fibroblasts, immune and endothelial cells, cytokines and growth factors levels (1), and by fewer and smaller adipocytes (2, 3). Collectively, these changes are termed desmoplasia.

Seminal studies demonstrated that the stroma contributes to tumor initiation, progression, and outcome. Tumor stromal cells (fibroblasts, adipocytes endothelial, and immune cells) promote epithelial cell proliferation, mutagenesis, angiogenesis, and migration and impair apoptosis and immunosurveillance (1, 4). Irradiation of mouse mammary gland stroma drives tumorigenesis of nonirradiated epithelial cells (5) and involuting mammary stroma facilitates progression of premalignant cells in xenografts (6, 7). Gene expression profiles of breast tumor–associated stroma are strongly associated with clinical outcome (8) and are remarkably similar to those of stroma surrounding ductal carcinomas *in situ* (DCIS; ref. 9), suggesting that tumor stroma develops early in tumorigenesis.

Selected desmoplastic features are also observed in nonmalignant breast tissues of women with high mammographic density (HD; refs. 1–3, 10, and 11). Mammographic density (MD) is determined by the relative amounts of radiolucent material (fat) and radiodense material (epithelial cells, fibroblasts and ECM) within the breast upon imaging. Radiodense areas, referred to as MD, exhibit histologic characteristics of malignant stroma, including low adipocyte content, high ECM, and stromal cell content (1–3, 10, 11). Women with MD > 75% have a 4- to 6-fold increase in invasive breast cancer compared with women with negligible MD (12, 13). It is estimated that almost one third of breast cancers may be attributable to high MD (13).

Previously, we showed that CD36 is necessary and sufficient to coordinately control adipocyte and matrix accumulation, two phenotypes that histologically define MD (3). CD36, a widely expressed transmembrane receptor, modulates cell type- and ligand-specific phenotypes, including adipocyte differentiation, angiogenesis, apoptosis, TGFβ1 activation, cell–ECM interactions, ECM deposition, and immune signaling

[1]Department of Pathology, University of California San Francisco, San Francisco, California. [2]Comprehensive Cancer Center, University of California San Francisco, San Francisco, California. [3]Lawrence Berkeley National Laboratory, Berkeley, California. [4]Department of Medicine, University of California San Francisco, San Francisco, California. [5]Department of Epidemiology, University of California San Francisco, San Francisco, California. [6]Department of Biostatistics, University of California San Francisco, San Francisco, California. [7]Department of Biomedical Engineering, University of Nevada, Reno, Nevada

Note: Supplementary data for this article are available at Cancer Research Online (http://cancerres.aacrjournals.org/).

R.A. DeFilippis and C. Fordyce contributed equally to this work.

Current address for R.A. DeFilippis: Department of Medicine, University of California San Francisco, San Francisco, California; current address for C. Fordyce, Department of Biochemistry and Molecular Biology, University of New Mexico, Albuquerque, New Mexico; and current address for K. Patten, Division of Biology & Biomedical Sciences, Washington University in St. Louis, St. Louis, Missouri.

Corresponding Author: Thea D. Tlsty, University of California San Francisco, 513 Parnassus, HSW 513, San Francisco, CA 94143. Phone: 415-502-6115; Fax: 415-502-6163; E-mail: Thea.Tlsty@ucsf.edu

doi: 10.1158/0008-5472.CAN-13-3390

(3, 14). CD36 expression is negligible in tumor stroma, in contrast to surrounding histologically disease-free tissue, and is inversely correlated with tumor size and grade (3). Strikingly, disease-free HD tissues (MD > 70%–75%) have reduced CD36 levels in multiple stromal components (adipocytes, endothelial cells, macrophages, and fibroblasts) compared with low mammographic density (LD) tissues (25% < MD < 50%), suggesting that CD36 repression is a multicellular coordinated stromal program active in tissues at high risk for tumorigenesis (3).

In addition to desmoplasia and HD, increased ECM is seen in other pathologic conditions associated with a DNA damage response (DDR) and/or telomere malfunction: fibrosis after γ-irradiation (15), dyskeratosis congenita (16), and pulmonary (17) and liver fibrosis (18). Previously, we demonstrated that DNA damaging agents and/or telomere malfunction in mortal, nontumorigenic variant human mammary epithelial cells (vHMEC) induce a DDR and activin A–dependent COX-2 expression (19). Fibroblasts from reduction mammoplasties (RMF) cocultured with DNA-damaged vHMEC induce many genes consistent with a desmoplastic phenotype (e.g., ECM and inflammatory cytokines) and activin A secretion by damaged vHMEC is necessary and sufficient for this induction (20). *In vivo*, DCIS lesions whose epithelial cells exhibit shorter telomeres, increased activin A and COX-2, are surrounded by activated fibroblasts and increased immune infiltrate (20), suggesting that microenvironmental alterations, mimicking aspects of desmoplasia, occur even in the absence of an invasive tumor.

This manuscript presents *in vitro* and *in vivo* data supporting our hypothesis that HD is generated by factors(s) secreted by DNA-damaged epithelial cells (including damage caused by shortened telomeres) that repress CD36 causing induction of desmoplastic-like phenotypes in adjacent fibroblasts.

Materials and Methods

Human subjects

Human tissues were accrued after informed consent and studied under institutionally approved protocols 10-02471 and 10-03756.

Human tissue analysis

Paraffin-embedded serial tissue sections, from 13 LD (25% < MD < 50%) and 14 HD (MD > 70%) disease-free women (Supplementary Table S1), were assessed for γH2AX levels by immunohistochemistry (3) and for telomere content by telomere-specific FISH (20). For immunohistochemistry, antigen retrieval was performed in citrate buffer (pH 6.0) for 30 minutes at 93°C before incubation with a γH2AX antibody (1:800; Millipore, #05-636) for 60 minutes at room temperature. For FISH, telomere-specific (Cy3-labeled) and centromere-specific (FITC-labeled) peptide nucleic acid probes were hybridized to tissue sections and the telomere to centromere intensity ratio calculated.

Isolation and propagation of human mammary epithelial cells and fibroblasts from disease-free tissues

Human mammary epithelial cells (HMEC) and vHMEC, which have silenced p16 (21), isolated from 12 biopsies of known MD (LD-HMEC/vHMEC or HD-HMEC/vHMEC; Supplementary Table S2) and four RMF (Supplementary Table S3), and human mammary fibroblasts (HMF), isolated from 14 biopsies of known MD (LD-HMF or HD-HMF; Supplementary Table S2) and 10 RMF (Supplementary Table S3), were propagated in MEGM and RPMI-1640 + 10% FBS, respectively (3, 4, 22, 23).

Etoposide treatment

LD-vHMEC and HD-vHMEC exposed to 50 μmol/L etoposide or vehicle control (DMSO) for 24 hours were assessed for γH2AX intensity and foci number, cell viability, apoptosis, and proliferation 0, 1, 3, 6, 12, and 24 hours after drug removal. Immunofluorescence detection of γH2AX was performed using the γH2AX antibody above (1:500; ref. 20). Cell viability (fraction of live/dead cells) and apoptosis (caspase 3/7 activity) were measured using an ApoTox-Glo Triplex Assay (Promega) and proliferation (BrdUrd incorporation) using the Cell Proliferation Assay Kit (Cell Signaling Technology). LD-vHMEC and HD-vHMEC exposed to 20 μmol/L etoposide or vehicle for 3 hours were assessed for long-term survival in a colony-formation assay 9 days after drug removal, and the surviving fractions (plating efficiency of cells exposed to etoposide/plating efficiency of cells exposed to vehicle) calculated (24).

Telomere-content assays

Telomere content was assessed with genomic DNA isolated from HMEC, vHMEC, and HMF using quantitative polymerase chain reaction (qPCR) as described (25). Telomeric DNA was expressed as the ratio of telomere cycle threshold (Ct) to the Human β globin gene Ct. Each sample was run in triplicate wells on each plate and averaged. Each target was analyzed in triplicate plates.

qPCR

qPCR was performed on a CFX-96 thermocycler using SsoFast Master Mix (BioRad) and TaqMan primer probe sets for each gene (Applied Biosystems) and the data analyzed using the standard curve method. Expression of β-D-glucuronidase (*GUSB*) was used to normalize for variances in input cDNA. For all experiments, each sample was run in triplicate wells on each plate and averaged, and each gene was analyzed in triplicate plates.

Treatment of RMF with conditioned media

LD-vHMEC and HD-vHMEC were plated in MEGM and conditioned their media for 48 hours. RMF were plated in RPMI-1640 + 10% FBS and grown for 24 hours in RPMI-1640 + 1% FBS before the media were replaced by a 1:1 mix of RPMI-1640 + 2% FBS and conditioned media (or control unconditioned media). RNA was isolated from RMF 48 hours after treatment with conditioned media.

ELISA

vHMEC were plated in MEGM and conditioned their media for 26 hours. Activin A and TGFβ1 protein levels were measured in the conditioned media using Duo-Set ELISA Kits #DY338 and DY420, respectively (R&D Systems).

Treatment of RMF

RMF, plated in RPMI-1640 + 10% FBS, were grown for 24 hours in RPMI-1640 without serum before the addition of:

activin A (Sigma-Aldrich); prostaglandin E2 (Cayman Chemicals); COX-2 inhibitor, NS398 (Cayman Chemicals); protein kinase A (PKA) inhibitor, H89 (Sigma-Aldrich); phosphatidylinositol 3-kinase (PI3K) inhibitor, LY294002 (Sigma-Aldrich); TGFβ receptor 1 (TGFβR1) inhibitors, LY364947 and SB431542 (Sigma-Aldrich); p38 mitogen-activated protein kinase (p38 MAPK) inhibitor SB203580 (Sigma-Aldrich); and MAPK kinase (MAPKK) inhibitor, UO126 (Sigma-Aldrich).

Coculture experiments

RMF were plated in 0.4-μm pore Transwell dishes (Costar) and cocultured with vHMEC expressing either control luciferase short hairpin (sh-luciferase), activin A short hairpin (sh-activin A), vector control, TRF2, or hTERT (19, 20). RNA was isolated from RMF 48 hours after initiation of coculture.

Immunocytochemistry

Immunocytochemistry was performed in RMF using primary antibodies against CD36 (1:20, #9154; Santa Cruz Biotechnology), fibronectin (1:100, #610077; BD Transduction), and α-smooth muscle actin (αSMA; 1:50, #M0851; Dako; ref. 3).

Adipocyte differentiation experiment

RMF, plated in RPMI-1640 + 10% FBS, were grown for 24 hours in RPMI-1640 without serum before exposure to 80 ng/mL activin A for 48 hours. The media were then replaced with RPMI-1640 + 10% FBS, ±80 ng/mL activin A and ±10 μmol/L 15-deoxy-D12,14-prostaglandin J2 (PJ2; Cayman Chemical) to induce adipocyte differentiation. Lipid accumulation was assayed after 1 week by Oil Red O staining (3).

Statistical and image analysis

Image acquisition, statistical analysis, and image analysis are described in Supplementary Methods.

Results

HD breast tissues have increased basal γH2AX and shortened telomeres compared with LD breast tissues

We hypothesized that HD epithelial cells have an elevated DDR and secrete factor(s) that repress CD36 expression and reprogram adjacent fibroblasts. To test this hypothesis, levels of γH2AX, a DNA damage marker, were assessed by immunohistochemistry (Fig. 1A, left) in biopsies obtained from disease-free women with measured MD (Supplementary Table S1). HD tissues had higher γH2AX levels (1.9-fold, $P < 0.0001$) than LD tissues (Fig. 1A, right and Supplementary Fig. S1A). To determine whether the increased DDR observed in HD tissues was associated with telomere malfunction, telomere DNA content was assessed by FISH (Fig. 1B, left). Telomere DNA content was reduced (1.2-fold,

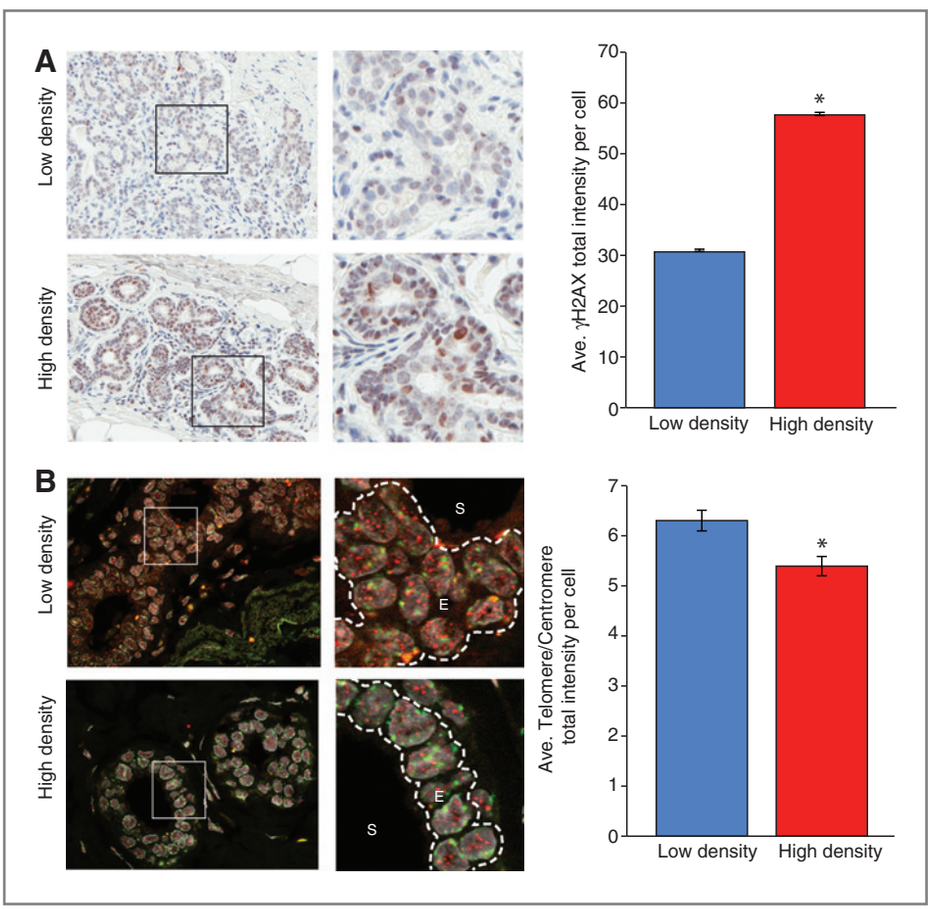

Figure 1. HD breast tissues have increased basal γH2AX and shortened telomeres compared with LD breast tissues. γH2AX protein levels and telomere content assessed by immunohistochemistry and FISH, respectively, in serial paraffin breast tissue sections from 13 LD and 14 HD disease-free women. A, left, representative bright field images (original magnification, ×20) of paraffin sections from 12 LD and 14 HD tissues stained for γH2AX (brown). Right, average and SEM of γH2AX intensity per cell. B, left, representative fluorescent images (original magnification, ×63) of paraffin sections from 12 LD and 11 HD tissues stained for telomere (red), centromere (green) and DNA (DAPI, gray). S, stromal cells; E, epithelial cells. Right, average and SEM of telomere signal/centromere signal per epithelial cell nucleus. *, $P < 0.0001$.

$P < 0.0001$) in HD epithelial cells compared with LD epithelial cells (Fig. 1B, right and Supplementary Fig. S1B). CD36 levels, measured by immunohistochemistry in this cohort, were lower (4.5-fold, $P < 0.0001$) in HD tissues than LD tissues (3). These *in vivo* data are consistent with our hypothesis that factors secreted by DNA-damaged HD epithelial cells repress CD36 in adjacent fibroblasts.

HD epithelial cells exhibit increased γH2AX, decreased proliferation, and shortened telomeres compared with LD epithelial cells

To further assess the differences between LD and HD tissues *in vitro*, we isolated and propagated 3 cell types (3, 4, 22, 23) from biopsies of disease-free women with measured MD (Supplementary Table S2): (i) human mammary epithelial cells (HMEC) with an intact p16/Rb pathway; (ii) vHMEC with a compromised p16/Rb pathway; and (iii) human mammary fibroblasts (HMF). We primarily used vHMEC for these experiments because: (i) HMEC have limited proliferative capability (~10 population doublings) compared with vHMEC (~30–65 population doublings); (ii) HMEC, which have intact cell-cycle checkpoints (p16/Rb), undergo growth arrest upon telomere malfunction, whereas vHMEC, which lack p16, still proliferate (19, 22); and (iii) vHMEC preexist *in vivo* in disease-free breast tissue (21).

To determine whether HD-vHMEC had a heightened basal DDR, as observed *in vivo*, basal γH2AX levels were measured. γH2AX levels were slightly higher (1.1-fold, $P = 0.05$) in HD-vHMEC than LD-vHMEC (Fig. 2A, left and Supplementary Fig. S2A). Cell propagation in culture leads to selective expansion of cells capable of surviving and proliferating. Therefore, cells with the most pronounced DDR and the highest levels of γH2AX ("jackpots") are likely lost from the population, potentially explaining why the difference in γH2AX levels between LD and HD cells is greater *in vivo* than *in vitro*. One might predict that "jackpots" would exist transiently in culture and in greater numbers in HD-vHMEC. To assess this possibility, cells with the 0.5% highest γH2AX levels ("jackpots") were counted.

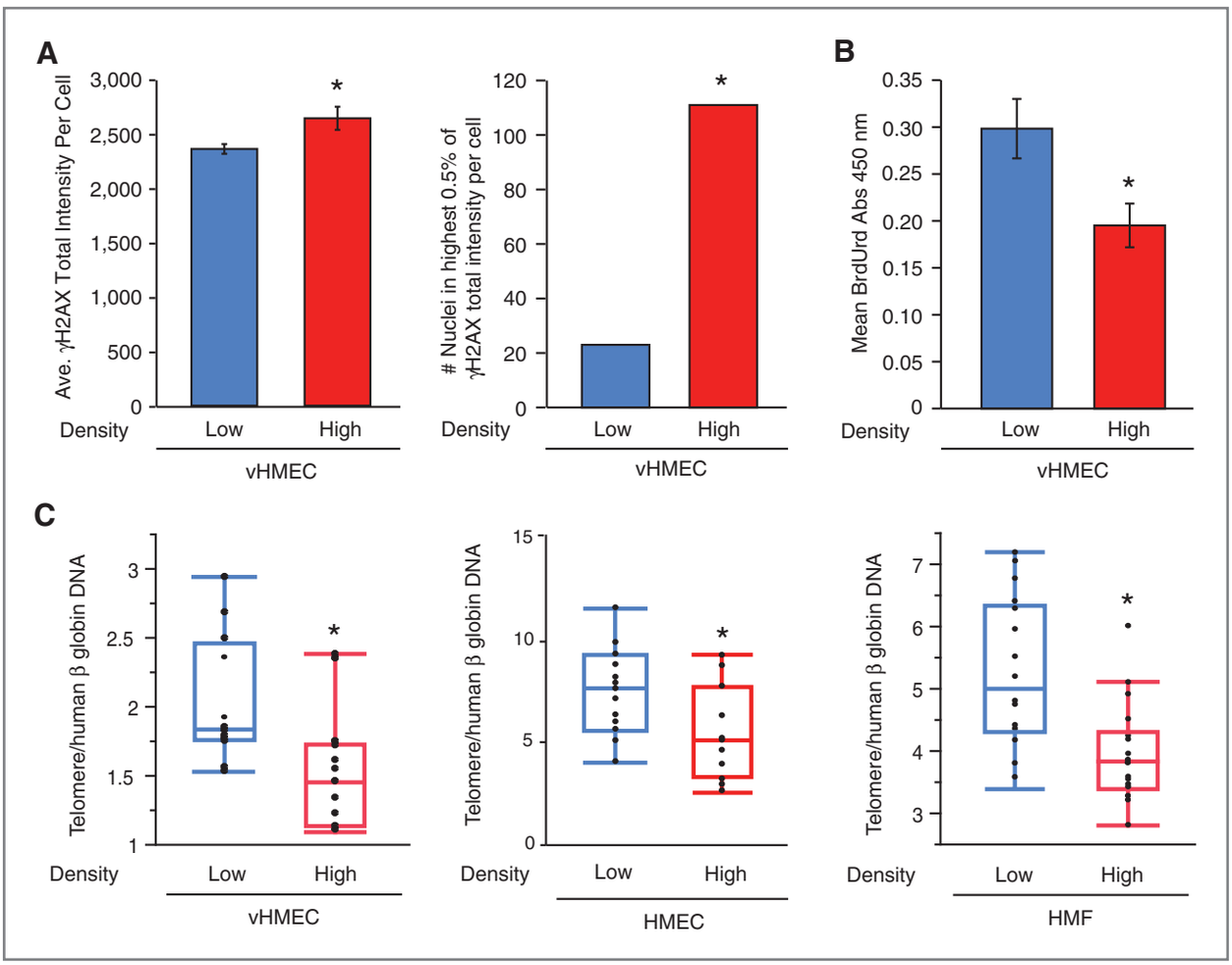

Figure 2. HD-vHMEC exhibit increased γH2AX, decreased proliferation, and shortened telomeres compared with LD-vHMEC. A, average and SEM of basal γH2AX intensity per nucleus (left) and number of nuclei with the highest 0.5% γH2AX intensity (right) in three LD-vHMEC and three HD-vHMEC. *, $P = 0.05$. B, average and SEM of basal BrdUrd incorporation, measured by absorbance at 450 nm, in six LD-vHMEC and six HD-vHMEC. *, $P = 0.01$. C, quantitation of telomere qPCR data for vHMEC (4 LD and 5 HD, left; *, $P = 0.007$). HMEC (5 LD and 4 HD, middle; *, $P = 0.03$), and HMF (6 LD and 4 HD, right; *, $P = 0.0009$).

"Jackpots" were more frequent (4.8-fold, $P < 0.0001$) in HD-vHMEC, as predicted (Fig. 2A, right).

Because the induction of a DDR typically leads to growth arrest or apoptosis, we asked whether HD-vHMEC showed reduced proliferation and/or increased apoptosis when compared with LD-vHMEC. HD-vHMEC showed decreased proliferation (1.5-fold, $P = 0.01$) when assessed by BrdUrd incorporation (Fig. 2B) but no significant difference in apoptosis when assayed for caspase-3/-7 activity (Supplementary Fig. S3B).

To determine whether HD epithelial cells had reduced telomere content, as observed *in vivo*, telomere DNA was measured by qPCR in LD and HD vHMEC, HMEC, and HMF (all at comparable population doublings: see Supplementary Fig. S2B and Supplementary Methods). Telomere DNA was reduced 1.4-fold in both HD-vHMEC and HD-HMEC compared with LD-vHMEC and LD-HMEC ($P = 0.007$ and 0.03, respectively; Fig. 2C, left and middle, respectively) and 1.3-fold in HD-HMF compared with LD-HMF ($P = 0.0009$; Fig. 2C, right), demonstrating that this phenotype is not restricted to the epithelial compartment. These *in vitro* data demonstrate that HD-vHMEC have increased basal γH2AX levels, reduced proliferation, and reduced telomere content compared with LD-vHMEC, recapitulating our observations *in vivo* and indicating that LD and HD epithelial cells are intrinsically distinct.

HD-vHMEC exposed to exogenous DNA damage exhibit enhanced γH2AX levels and viability compared with LD-vHMEC

To assess whether HD-vHMEC have a differential response to exogenous DNA damage, LD-vHMEC and HD-vHMEC were exposed to etoposide for 24 hours to induce double-strand DNA breaks, and γH2AX intensity quantitated (Fig. 3A). LD-vHMEC and HD-vHMEC exhibited increased γH2AX intensity after etoposide exposure (2.0-fold, $P < 0.0001$; 2.6-fold, $P < 0.0001$; respectively). However, γH2AX intensity was higher (1.4-fold, $P < 0.0001$) in HD-vHMEC.

To assess the ability of LD-vHMEC and HD-vHMEC to recover from etoposide-induced DNA damage, γH2AX levels were measured 0, 1, 3, 6, 12, and 24 hours after drug removal (Fig. 3B). HD-vHMEC consistently exhibited significantly higher γH2AX intensity than LD-vHMEC. Importantly, although γH2AX intensity in LD-vHMEC returned to basal levels by 12 hours, γH2AX intensity in HD-vHMEC remained elevated for 24 hours, suggesting that DNA repair is less efficient in HD-vHMEC.

Although γH2AX intensity is frequently used as a readout of DDR, and correlates well with the amount of DNA damage (26) and γH2AX foci (27), we nonetheless counted the number of γH2AX foci in a subset of LD-vHMEC and HD-vHMEC (Supplementary Fig. S3A). Consistent with γH2AX intensity measurements, both LD-vHMEC and HD-vHMEC exhibited increased γH2AX foci number (6.3-fold, $P < 0.0001$; 9.8-fold, $P < 0.0001$; respectively) after etoposide exposure. Furthermore, although not statistically significant, γH2AX foci number was higher in HD-vHMEC 0 and 24 hours after etoposide removal (1.1- and 1.4-fold, respectively).

Cell viability (Fig. 3C) and apoptosis (Supplementary Fig. S3B) were assessed 0, 1, 3, 6, 12, and 24 hours after etoposide removal. In spite of their increased and sustained DDR, HD-vHMEC exhibited increased cell viability compared with LD-vHMEC for the entire time course. Both LD-vHMEC and HD-vHMEC showed increased levels of apoptosis upon etoposide exposure. However, HD-vHMEC underwent less apoptosis than LD-vHMEC (although not statistically significant) for the entire time course, consistent with their increased viability. We also assessed the long-term survival of these cells after exposure to etoposide using a colony formation assay (Fig. 3D), and found that HD-vHMEC formed more colonies than LD-vHMEC 9 days after etoposide removal (2.2-fold, $P = 0.006$).

These *in vitro* data demonstrate that HD-vHMEC have elevated and persistent γH2AX levels, increased viability/survival and decreased apoptosis following exogenous DNA damage, compared with LD-vHMEC. Therefore, LD-vHMEC and HD-vHMEC have intrinsic differences in both their basal and induced DDR.

HD-vHMEC secrete factors that repress CD36 in RMF to a greater extent than LD-vHMEC

Having demonstrated that LD-vHMEC and HD-vHMEC are intrinsically different, we tested our hypothesis that secreted factor(s) from HD epithelial cells repress *CD36* expression in adjacent stromal cells. *CD36* mRNA levels were assessed in RMF (Supplementary Table S3) after exposure to control unconditioned media or conditioned media from LD-vHMEC or HD-vHMEC (Fig. 4A, left). Conditioned media from both LD-vHMEC and HD-vHMEC repressed *CD36* in RMF compared with unconditioned media (1.6-fold, $P < 0.0001$; 2.2-fold, $P < 0.0001$, respectively). However, consistent with our hypothesis, conditioned media from HD-vHMEC repressed CD36 in RMF more than conditioned media from LD-vHMEC (1.4-fold, $P = 0.0005$).

Activin A is upregulated in HD-vHMEC compared with LD-vHMEC

Induction of a DDR in vHMEC is associated with increased activin A (19). To assess whether the heightened DDR observed in HD-vHMEC was associated with higher activin A, activin A mRNA, and protein levels were measured in LD-vHMEC and HD-vHMEC. HD-vHMEC had higher levels of activin A mRNA (1.4-fold, $P = 0.03$) and protein (1.8-fold, $P = 0.04$) than LD-vHMEC (Fig. 4A, middle and right, respectively).

Activin A is a TGFβ family member and TGFβ is known to induce ECM accumulation/fibrosis (28). Therefore, we evaluated TGFβ1 protein levels in LD-vHMEC and HD-vHMEC and in vHMEC with increased telomere malfunction, that is, overexpressing TRF2 (TRF2-vHMEC), and vHMEC with reduced telomere malfunction, that is, overexpressing hTERT (hTERT-vHMEC; ref. 19). TGFβ1 protein levels were not significantly different between LD-vHMEC and HD-vHMEC nor between TRF2-vHMEC and hTERT-vHMEC (Supplementary Fig. S4A and S4B, respectively), demonstrating that TGFβ1 does not contribute to the DDR in vHMEC in our experimental conditions.

We previously showed that activin A, induced by DDR, is necessary and sufficient for COX-2 induction in vHMEC (19). As predicted, *COX-2* mRNA levels were higher (1.5-fold, $P = 0.09$) in HD-vHMEC than LD-vHMEC (Supplementary

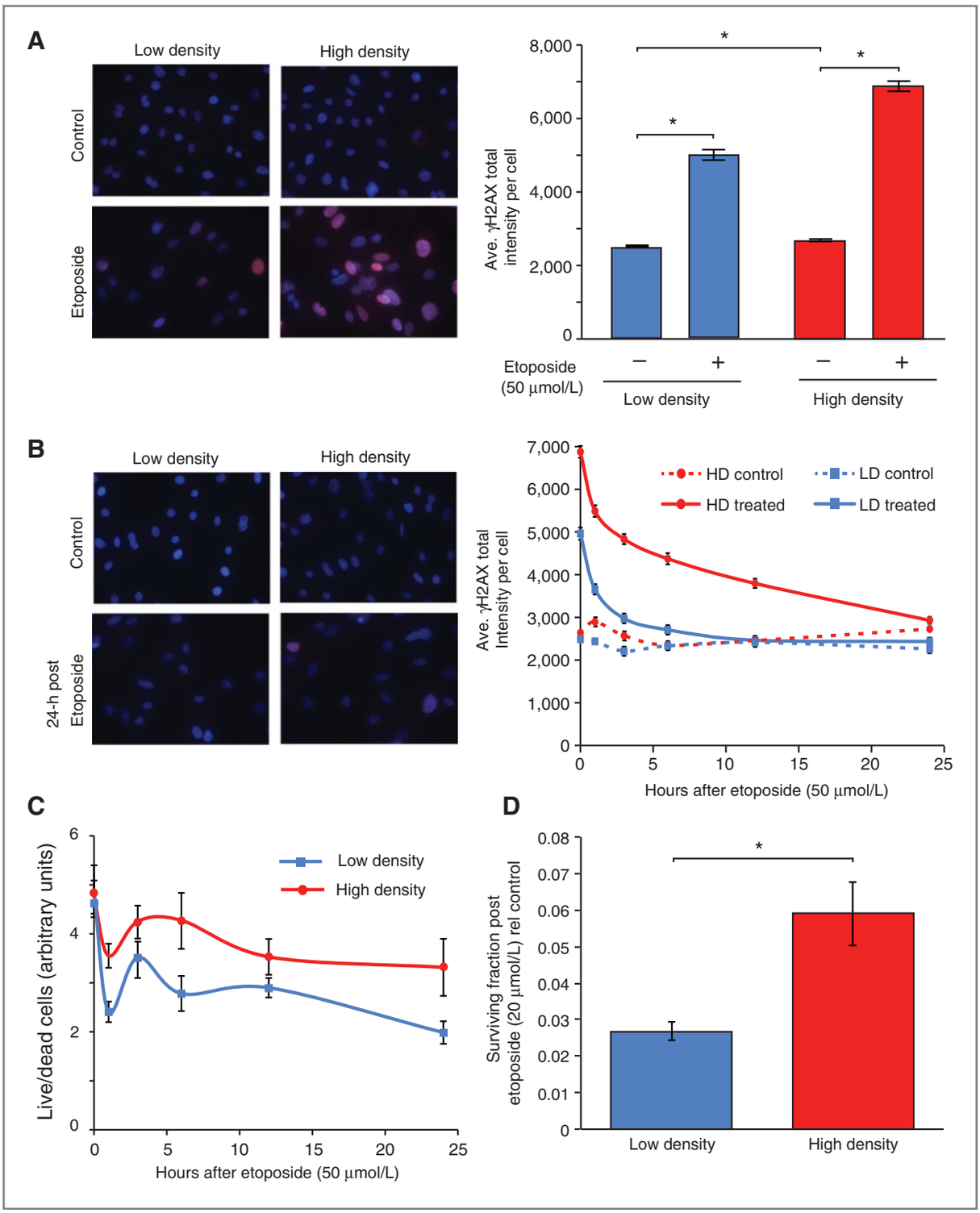

Figure 3. HD-vHMEC exposed to exogenous DNA damage exhibit increased γH2AX and increased viability/survival compared with LD-vHMEC. Three LD-vHMEC and three HD-vHMEC (A, B, and D) or six LD-vHMEC and six HD-vHMEC (C) exposed to 50 μmol/L etoposide for 24 hours (A, B, and C) or 20 μmol/L etoposide for 3 hours (D) were assessed for γH2AX intensity (A and B), cell viability (C), or long-term survival (D). A and B, left, representative fluorescent images (original magnification, ×10) of γH2AX staining (red) 0 hours (A) or 24 hours (B) after etoposide removal. A and B, right, average and SEM of γH2AX intensity per nucleus at 0 hours (A; *, $P < 0.0001$) or 1, 3, 6, 12, and 24 hours (B) after etoposide removal. C, average and SEM of cell viability (live/dead cells) 0, 1, 3, 6, 12, and 24 hours after etoposide removal. D, average and SEM of surviving fraction (plating efficiency of cells exposed to etoposide/plating efficiency of control cells) 9 days after etoposide removal. *, $P = 0.006$.

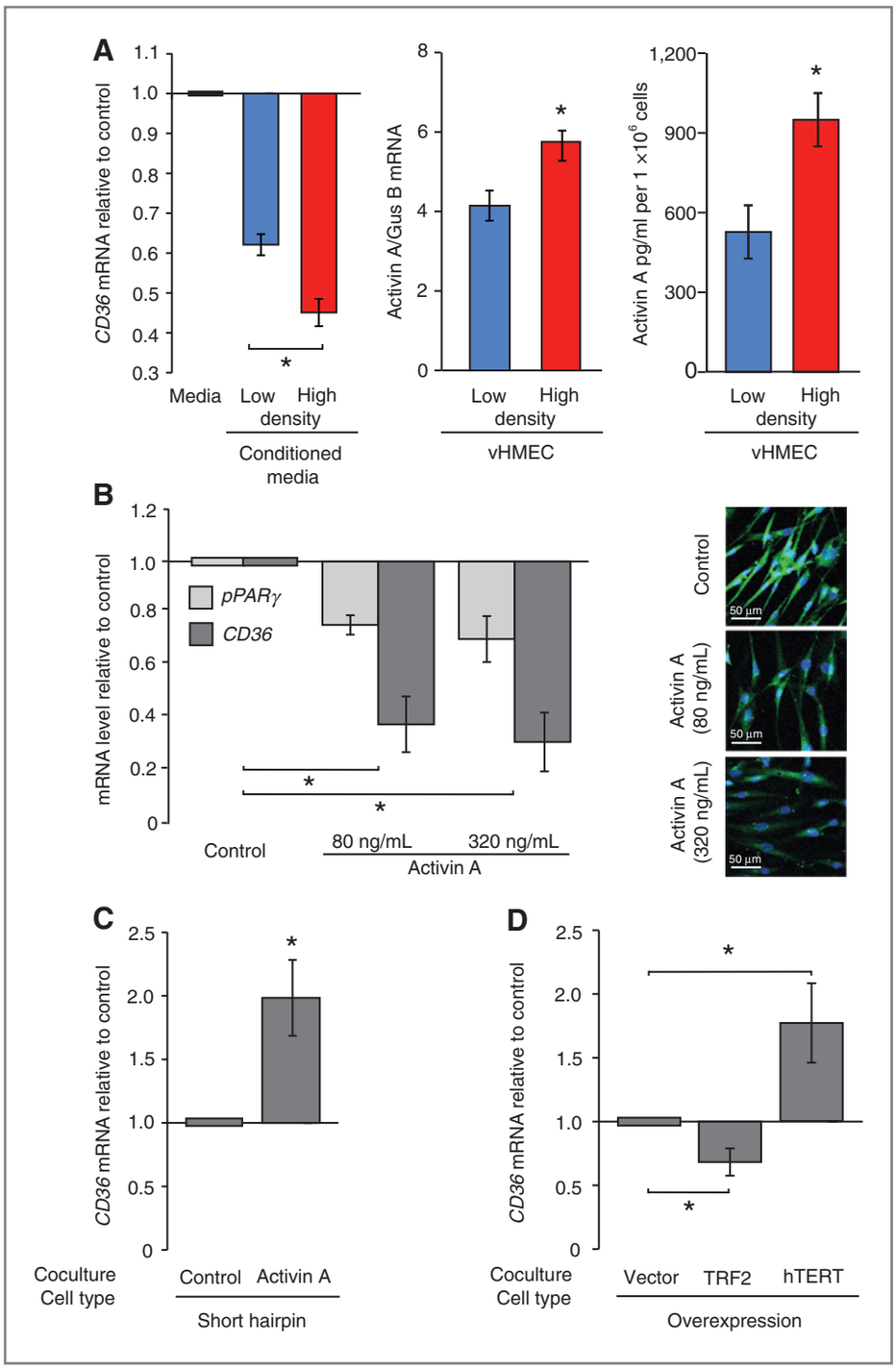

Figure 4. Shortened telomeres and increased activin A secretion in HD-vHMEC compared with LD-vHMEC is necessary and sufficient for CD36 repression in RMF. A, left, two RMF exposed for 48 hours to control unconditioned media, or media conditioned for 48 hours by five LD-vHMEC or five HD-vHMEC, were assayed for *CD36* mRNA by qPCR. Average and SEM of *CD36* mRNA fold change relative to RMF exposed to control medium in one RMF. *, $P = 0.0005$. Middle, average and SEM of *activin A* mRNA levels measured by qPCR in five LD-vHMEC and five HD-vHMEC. *, $P = 0.03$. Right, average and SEM of activin A protein levels measured by ELISA in six LD-vHMEC and four HD-vHMEC. *, $P = 0.04$. B, left, *CD36* and *PPARγ* mRNA levels were measured by qPCR in two RMF exposed to 80 ng/mL (*, $P = 0.01$, 0.0007) and 320 ng/mL (*, $P = 0.02$, 0.015) of activin A for 48 hours. Average and SEM of mRNA fold change relative to untreated RMF. Right, representative fluorescent images (original magnification, ×20) of CD36 protein staining (green) in one RMF exposed to 80 and 320 ng/mL of activin A for 48 hours. C and D, two RMF were cocultured with two vHMEC for 24 hours and assayed for *CD36* mRNA by qPCR. vHMEC expressed a short hairpin for luciferase (control) or for activin A (activin A; C; *, $P = 0.007$) or overexpressed mock (vector), TRF2 (*, $P = 0.01$) or hTERT (D; *, $P = 0.03$). Average and SEM of *CD36* mRNA fold change relative to RMF cocultured with control short hairpin (C) or vector control (D).

Fig. S4C). These data further support that the stress response previously identified by us in DNA-damaged vHMEC (19) is heightened in HD-vHMEC compared with LD-vHMEC.

Activin A and telomere malfunction in vHMEC are necessary and sufficient for CD36 repression in RMF

To determine whether activin A was sufficient to repress CD36 in RMF, RMF were exposed to 80 and 320 ng/mL activin A. Exposure to 80 ng/mL activin A repressed CD36 mRNA (2.6-fold, $P = 0.01$) and protein levels (Fig. 4B, left and right, respectively). A similar repression was observed at 320 ng/mL. Because CD36 expression is primarily controlled by the transcription factor PPARγ (29), we asked whether activin A–dependent CD36 repression could be mediated by PPARγ. RMF exposed to activin A repressed *PPARγ* mRNA at both doses (1.3-fold, $P = 0.007$; 1.4-fold, $P = 0.015$,

respectively; Fig. 4B, left). To assess whether activin A secretion by vHMEC was necessary for *CD36* repression in RMF, RMF were cocultured with vHMEC expressing short hairpin RNA to either a control (sh-Luciferase-vHMEC) or activin A (sh-activin A-vHMEC). RMF cocultured with sh-activin A-vHMEC had higher levels of *CD36* mRNA (2.0-fold, $P = 0.007$) than RMF cocultured with sh-luciferase-vHMEC (Fig. 4C). Thus, activin A is sufficient to repress CD36 in RMF and activin A secretion by vHMEC is necessary for CD36 repression in RMF.

Activin A induces COX-2 and secretion of its product, prostaglandin E2 (PGE2), in vHMEC (19). To ascertain whether COX-2 expression and PGE2 secretion by vHMEC was necessary and/or sufficient for *CD36* repression in RMF, RMF were exposed to activin A, PGE2, or a COX-2 inhibitor (NS398), or activin A and NS398 together and *CD36* mRNA levels measured (Supplementary Fig. S4D). *CD36* expression was repressed in RMF exposed to activin A, but exposure to PGE2 did not repress *CD36*. In addition, exposure of RMF to NS398 did not affect activin A–mediated *CD36* repression, demonstrating that COX-2 induction, and the subsequent secretion of PGE2, by vHMEC is neither necessary nor sufficient for *CD36* repression in RMF.

To evaluate whether telomere malfunction in vHMEC was necessary and/or sufficient for *CD36* repression in RMF, RMF were cocultured with vector-vHMEC (control), TRF2-vHMEC with increased telomere malfunction, or hTERT-vHMEC with reduced telomere malfunction (19). *CD36* mRNA levels were repressed in RMF cocultured with TRF2-vHMEC (1.5-fold, $P = 0.01$) but elevated in RMF cocultured with hTERT-vHMEC (1.8-fold, $P = 0.03$) compared with RMF cocultured with vector-vHMEC (Fig. 4D). These data demonstrate that telomere malfunction in vHMEC is necessary and sufficient for *CD36* repression in RMF and expand our previous report about cell-extrinsic consequences of telomere malfunction (20).

Transient exposure to activin A persistently represses CD36 in RMF

To gain further insights into the biologic relevance of CD36 regulation by activin A, we analyzed the sensitivity and durability of this regulation in RMF *in vitro*. RMF exposed to physiologic levels (~1.2 ng/mL) of activin A (30) for 48 hours showed *CD36* repression in a dose-dependent manner, repression being observed (1.4-fold, $P = 0.05$) with as little as 1.25 ng/mL of activin A (Fig. 5A). Exposure of RMF to two doses of activin A for 2, 4, or 8 days repressed *CD36* to a similar extent (2.6- to 3.4-fold, $P < 0.05$) under all conditions, demonstrating that a 2-day exposure to activin A is sufficient for maximum *CD36* repression in RMF (Fig. 5B). Importantly, RMF exposed to activin A for 48 hours then propagated in the absence of activin A for five passages exhibited sustained (and even increasing) *CD36* mRNA repression (1.3-fold, $P = 0.0006$ at P5) for several weeks after activin A removal (Fig. 5C and Supplementary Fig. S5). In summary, *CD36* expression in RMF is exquisitely sensitive to physiologic levels of activin A and even a brief exposure to activin A can result in prolonged *CD36* repression.

Activin A–dependent repression of CD36 requires activin A/TGFβ family type I receptor and MAPK pathways

To elucidate the mechanism(s) by which activin A represses *CD36* in RMF, RMF were exposed to activin A alone or in the presence of various pathway inhibitors or vehicle control (control RMF; Fig. 5D). Activin A, like other TGFβ family members, signals through the TGFβ family type I and type II receptors. We found that RMF exposed to activin A plus TGFβ family type I receptor (TGFβR1) inhibitors (LY364947 and SB431542) exhibited higher levels of *CD36* (5.7-fold, $P = 0.0001$; 5.8-fold, $P < 0.0001$, respectively) than control RMF, demonstrating that activin A/TGFβR1 signaling is required for activin A–dependent *CD36* repression. Previous studies demonstrated that MAPK represses *CD36* and that activin A utilizes the MAPK pathway (19, 31). RMF exposed to activin A plus MAPK kinase (MAPKK) inhibitor (UO126) had higher *CD36* levels (2.9-fold, $P = 0.004$) than controls. Thus, the MAPK pathway is necessary for activin A–dependent *CD36* repression. In contrast, RMF exposed to activin A plus PI3K inhibitor (LY294002) exhibited lower *CD36* levels (1.8-fold, $P < 0.0001$) than controls, suggesting that the PI3K pathway is required for the induction of *CD36* expression. Finally, RMF exposed to activin A plus PKA inhibitor (H89) or activin A plus p38 MAPK inhibitor (SB203580) had similar levels of *CD36* to controls, demonstrating that neither of these pathways are involved in regulating *CD36* expression in this context.

Activin A modulates CD36-dependent phenotypes

If a DDR and increased activin A secretion in HD epithelial cells was responsible for the CD36-modulated desmoplastic-like phenotypes (low adipocyte and high ECM content) observed in HD tissues *in vivo* (3), activin A should modulate these phenotypes in RMF *in vitro*.

RMF were placed under proliferative or adipocyte differentiation conditions, in the absence or presence of activin A, and Oil Red O staining, an indicator of intracellular fat accumulation, was measured (Fig. 6A; ref. 32). RMF grown in the absence or presence of activin A both accumulated fat under differentiation conditions compared with proliferative conditions (15.7- and 25.4-fold, respectively, $P < 0.0001$). However, RMF exposed to activin A accumulated significantly less fat under differentiation conditions than RMF grown without activin A (1.2-fold, $P < 0.0001$).

RMF were exposed to two doses of activin A and protein and mRNA levels for selected ECM genes were assessed. Exposure of RMF to activin A induced fibronectin and α-SMA protein accumulation (Fig. 6B, left) and *tenascin C, fibronectin*, and *collagen 1A1* mRNAs (4.1-fold, $P = 0.0004$; 1.8-fold, $P = 0.025$; 1.7-fold, $P = 0.012$; respectively, for 80 ng/mL; Fig. 6B, right) similarly at both doses. Thus, activin A can decrease fat accumulation and increase matrix accumulation in RMF *in vitro*, two prominent phenotypes of HD tissue modulated by CD36 expression.

Discussion

We previously showed, *in vitro* and *in vivo*, that CD36 is dramatically repressed in multiple stromal cell types within disease-free tissues from women with HD compared with

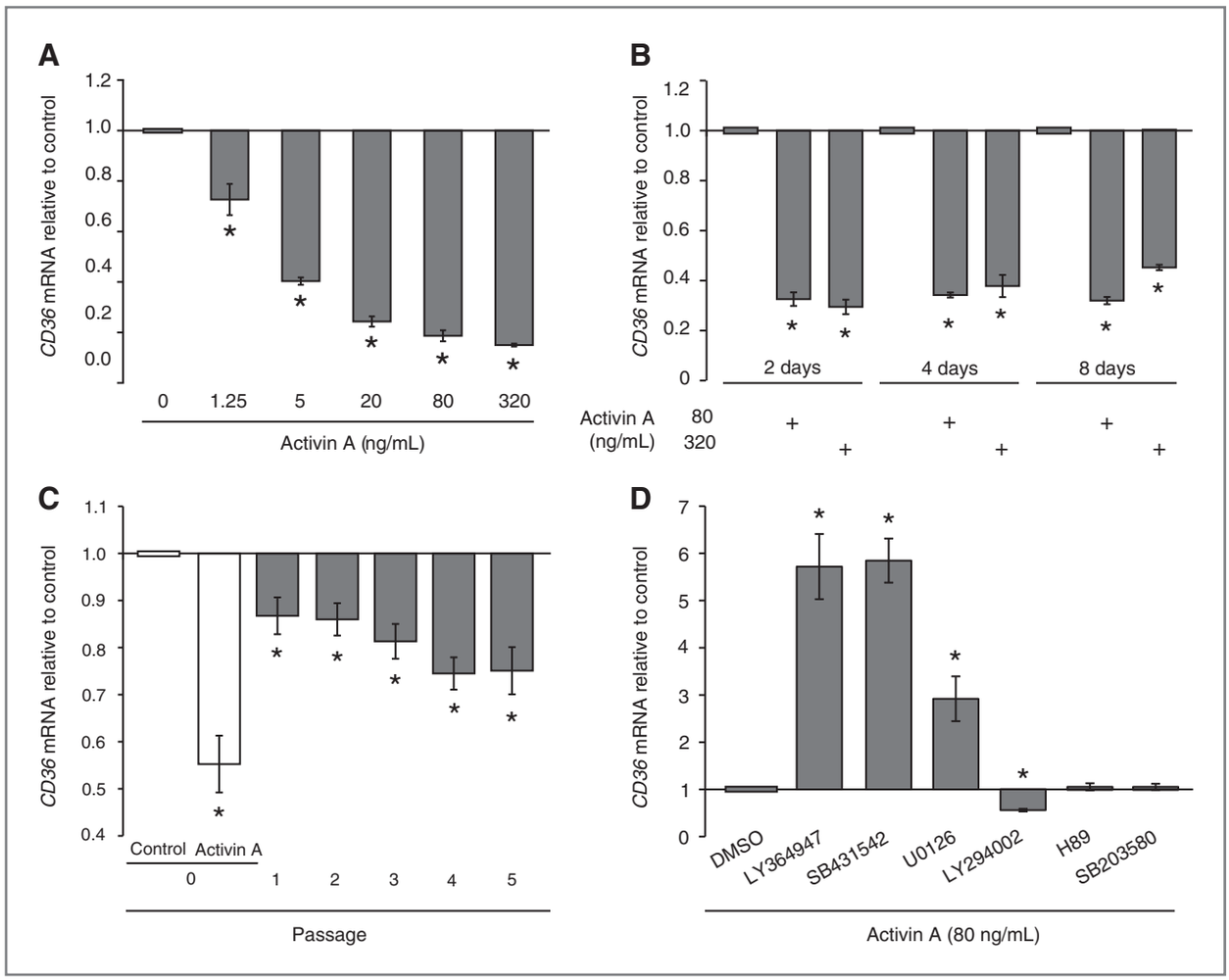

Figure 5. Activin A represses *CD36* in RMF, at low doses and persistently, in a TGFβR and MAPK-dependent manner. A–D, average and SEM of *CD36* mRNA fold change relative to control cells, measured by qPCR. A, one RMF exposed to the indicated doses of activin A for 48 hours. *, $P = 0.05$, 0.0006, 0.0007, < 0.0001. B, two RMF exposed to 80 and 320 ng/mL of activin A for 2, 4, or 8 days. C, four RMF were exposed to activin A (80 ng/mL) for 48 hours and *CD36* mRNA levels were determined immediately after exposure (P0; *, $P < 0.0001$) and for five passages (P1–P5; *, $P = 0.006$, 0.002, 0.0004, < 0.0001, 0.0006, respectively) after activin A removal. D, three RMF were exposed for 48 hours to activin A (80 ng/mL) alone or in the presence of DMSO vehicle control or 10 μmol/L various pathway inhibitors: TGFβR1 inhibitors [LY364947 (*, $P = 0.0001$) and SB431542 (*, $P < 0.0001$)], MAPKK inhibitor (UO126; *, $P = 0.004$), PI3K inhibitor (LY294002; *, $P < 0.0001$), PKA inhibitor (H89), or p38 MAPK inhibitor (SB203580).

women with LD (3). To define the mechanisms that account for CD36 repression, we tested the hypothesis that HD results from stress signaling in epithelial cells that induces the secretion of factors that repress CD36 and reprogram adjacent fibroblasts. Using cohorts previously used by us to study CD36-dependent phenotypes (3), we show that HD epithelial cells have more basal DNA damage (γH2AX intensity) than LD epithelial cells. In addition, HD-vHMEC have more γH2AX foci after exogenous DNA damage, and take longer to resolve these foci, than LD-vHMEC. Paradoxically, HD-vHMEC also have increased viability/survival and decreased apoptosis after exogenous DNA damage, a property that could facilitate the escape of a mutated clone, leading to cancer. HD epithelial cells also have slightly shorter telomeres, both *in vitro* and *in vivo*, than LD epithelial cells. This relatively small difference is not surprising because telomere length is a tightly regulated phenotype.

We previously reported that DNA damage or telomere malfunction in epithelial cells results in increased secretion of activin A, which can act in a paracrine or autocrine fashion to induce its own expression, and the expression of many protumorigenic genes, in adjacent cells (19, 20). Similarly, we find that HD-vHMEC, with increased DNA damage, have higher activin A levels than LD-vHMEC. We describe a novel phenotype associated with this pathway by showing that *CD36* expression in RMF is exquisitely sensitive to physiologic levels of activin A (30), and that even a transient exposure to activin A can persistently repress *CD36*. Consistent with our hypothesis, conditioned media from HD-vHMEC are more potent in repressing *CD36* in RMF than conditioned media from LD-vHMEC. Activin A and telomere malfunction in vHMEC are

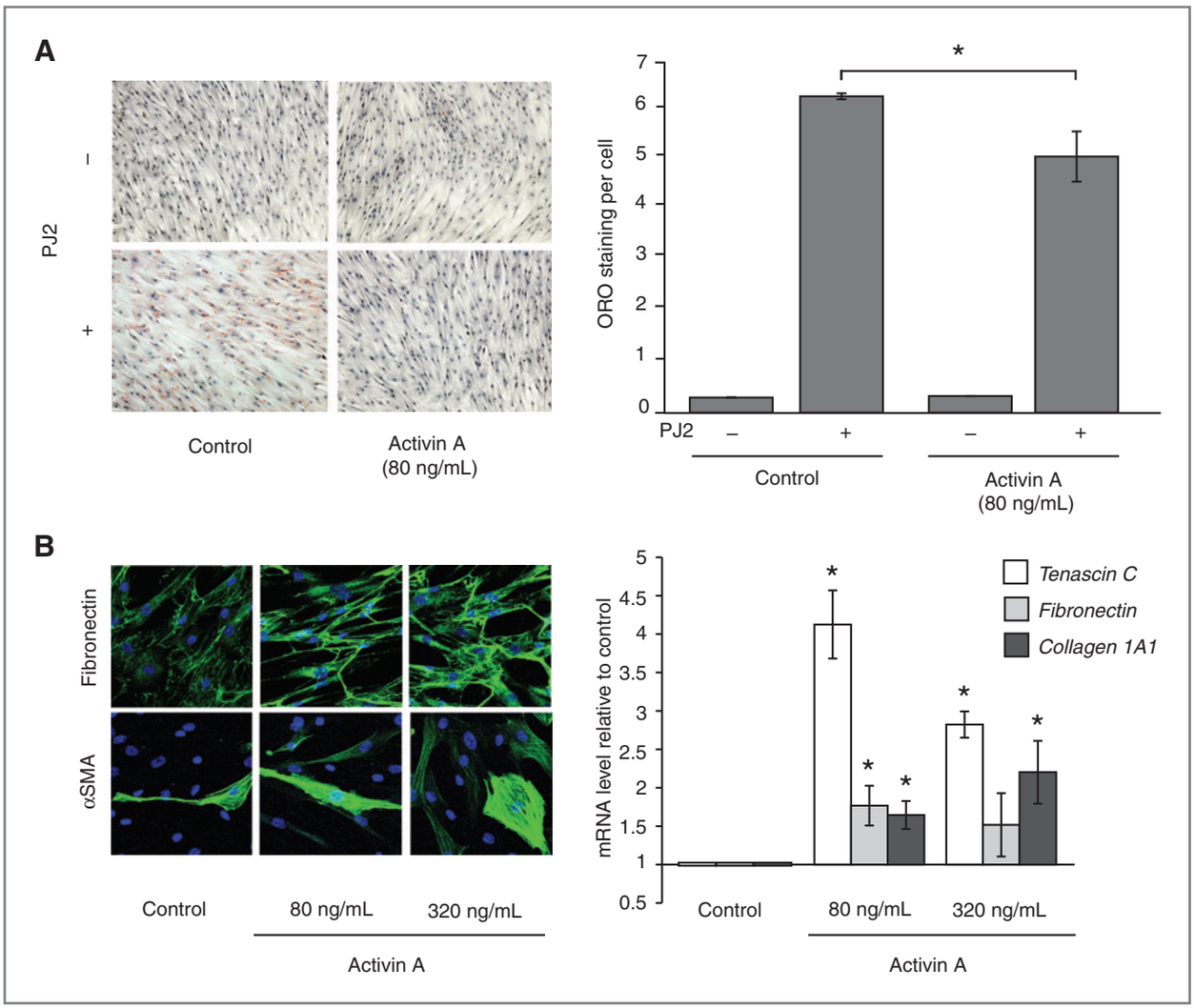

Figure 6. Activin A modulates CD36-dependent phenotypes *in vitro*. A, left, representative bright field images (original magnification, ×10) of two RMF placed under proliferative (−PJ2) or adipocyte differentiation (+PJ2) conditions, in the absence (control) or presence of activin A (80 ng/mL), for 7 days and assessed for adipocyte formation by Oil Red O staining (red). Right, average and SEM of Oil Red O staining per cell in one RMF. *, $P < 0.0001$. B, two RMF were exposed to 80 and 320 ng/mL of activin A for 48 hours. Left, representative fluorescent images (original magnification, ×20) of fibronectin (top) and αSMA (bottom) protein staining (green). Right, average and SEM of tenascin C (*, $P = 0.004$, 0.02), fibronectin (*, $P = 0.03$, 0.298), and collagen 1A1 (*, $P = 0.01$, 0.04) mRNA fold change relative to untreated RMF, measured by qPCR.

both necessary and sufficient for this repression. Importantly, activin A also modulates CD36-dependent desmoplastic-like phenotypes *in vitro*.

Our data suggest that CD36 repression may result from epigenetic modification, in addition to repression of its key regulator PPARγ. First, HD-HMFs maintain *CD36* repression in culture over several passages in the absence of exogenous activin A or interaction with HD epithelial cells (3). In addition, exposure to trichostatin A, a histone deacetylase inhibitor, increases *CD36* expression more extensively in HD-HMF than LD-HMF (unpublished data). Finally, transient exposure to activin A persistently represses *CD36* expression in RMF. Hence, even transient DNA damage in epithelial cells, and the subsequent secretion of activin A, could result in prolonged *CD36* repression in adjacent fibroblasts.

We demonstrate that the activin A–dependent repression of *CD36* in RMF requires both the activin A receptor (TGFβRI) and MAPK pathways, consistent with reports demonstrating that MAPK can regulate PARγ function and repress CD36 (31) and with activin A's ability to repress PPARγ expression in RMF. Although TGFβ1 has been implicated in CD36 repression in macrophages (31), TGFβ1 levels are not elevated in HD-vHMEC, nor in vHMEC with telomere malfunction, suggesting that TGFβ1 does not participate in *CD36* repression in this context. Finally, we show that, unlike many other protumorigenic phenotypes previously described by us (19, 20), *CD36* repression in RMF is not COX-2 dependent.

We envision a scenario in which (i) elevated basal DNA damage in HD epithelial cells results in increased activin A secretion; (ii) activin A binds to its receptor on adjacent

fibroblasts and activates the MAPK pathway; (iii) MAPK pathway activation results in PPARγ phosphorylation and inhibition; (iv) PPARγ inhibition leads to decreased *CD36* transcription and subsequently, the induction of the desmoplastic-like phenotypes observed in HD tissues (Fig. 7). In response, and as an extension, these desmoplastic-like fibroblasts can in turn promote motility of neighboring epithelial cells (20) and induce DNA damage of neighboring epithelial cells through the release of reactive oxygen species (ROS; ref. 33). Damaged epithelial cells would further exacerbate protumorigenic fibroblast phenotypes via the induction of activin A–dependent signaling pathways, thus propagating the DNA damage signal and the associated HD phenotypes throughout the tissue. Therefore, a breast with more DNA-damaged epithelial cells would exhibit more mammographically dense areas, leading to overall high MD. Our study highlights the reciprocal interactions between epithelial and stromal cells and their potential to induce carcinogenic processes and shows, for the first time, that there is a differential level of this cellular cross-talk in LD and HD tissues. The model described above suggests that these reciprocal interactions are initiated by a DNA damage event in the epithelial compartment. However, we cannot rule out that the initiating event occurs in the stromal compartment or, alternatively, simultaneously in both epithelial and stromal compartments. Regardless of the source of the initiating event, our data suggest that the alterations in LD and HD epithelial cells and fibroblasts are "intrinsic" and subsequently maintained in cells purified from tissues and propagated *in vitro*.

Our data support one potential mechanism that contributes to MD (Fig. 7). However, MD is a complex phenotype likely regulated by multiple pathways. Studies have implicated IGF1 in the acquisition of HD (10). Interestingly, *IGF1* mRNA levels are higher (2-fold, $P = 0.09$) in HD-HMF than LD-HMF and activin A induces *IGF1* expression (5.7- to 6.5-fold, $P = 0.0002$) in RMF (unpublished data). In addition, although we ruled out the involvement of TGFβ1 in the DDR pathway, TGFβ1 could be involved in another context because it promotes fibrosis (28), a phenotype exhibited by HD.

MD is a heritable trait that can be modified by environmental factors (34). The same can be said of telomere length; for example, chronic stress is correlated with shortened telomeres (35, 36). We, and others, have demonstrated that loss of telomere DNA can have cell-extrinsic consequences that may facilitate the development of a protumorigenic stroma (20, 37). This may partially explain why loss of telomere DNA is associated with poor clinical outcome for women with breast cancer and increased risk of cancer (38, 39). This study is the first to suggest that telomere malfunction also contributes to HD.

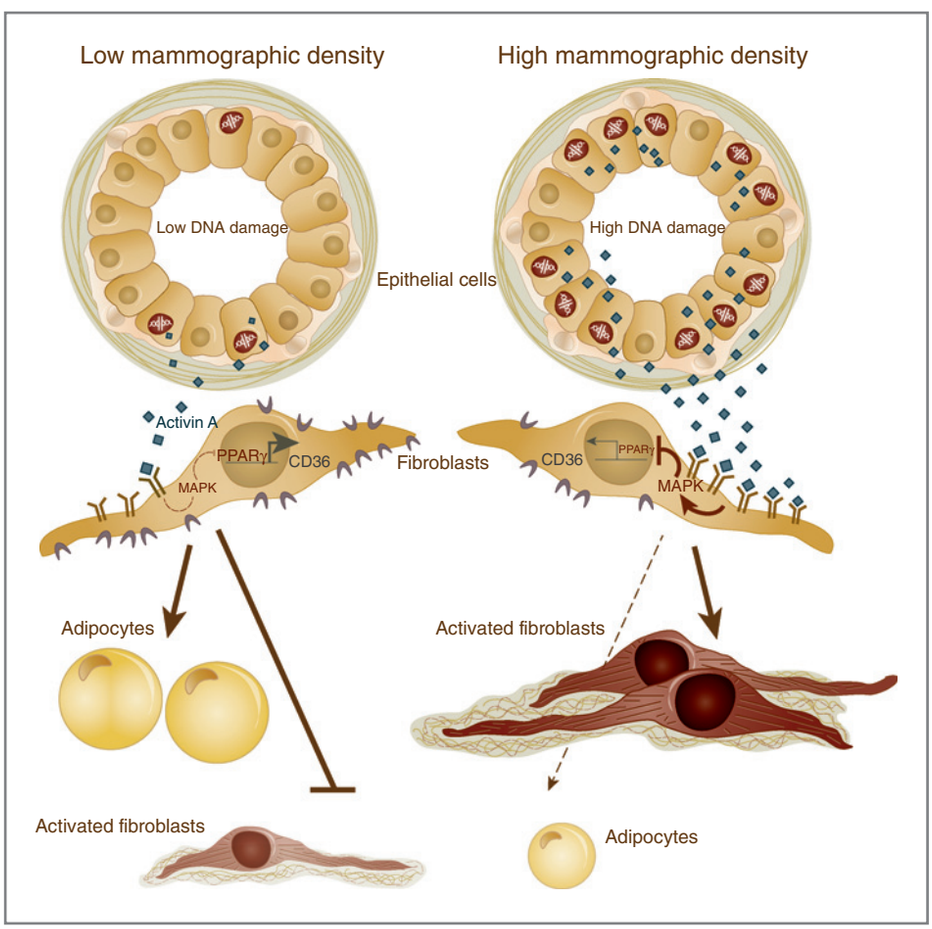

Figure 7. Proposed model depicting the cross-talk between epithelial cells and fibroblasts in LD and HD tissues. Arrows and bars indicate induction or repression, respectively, of gene expression, protein activity, or phenotypes. Solid and dotted lines indicate a strong or blunted/weak effect, respectively. Activin A and CD36 proteins are represented by diamonds or crescents, respectively.

In the breast, sex hormones drive expansion and involution of epithelial cells during menstrual cycling and lactation. Provocatively, expansion of epithelial cells during the luteal phase of the menstrual cycle is accompanied by modest but significant increases in MD (40) and coincides with the highest serum activin A levels (41). Successive expansion and involution may leave epithelial cells particularly vulnerable to DNA damage or telomere malfunction and select for genetically unstable cells able to resist apoptosis, like HD-vHMEC.

One might anticipate that as women age and their telomeres shorten, increased stress signaling would drive an increase in MD. However, MD remains the same or even decreases with age (42). This apparent contradiction could be explained by age-related lobular involution. This age-dependent loss of mammary epithelial cells would translate into decreased signaling to adjacent fibroblasts and a concomitant decrease in production of HD phenotypes. In fact, there is an inverse relationship between age-related involution and both MD and breast cancer risk (43, 44).

The demonstration that decreasing MD reduces breast cancer risk (45) provides tremendous opportunities for cancer prevention. Several drugs in clinical trials or already approved by the Federal Drug Administration modulate potential therapeutic targets identified in this study. Activin A is inhibited by competitive inhibitors of its receptor (e.g., bimagrumab), soluble receptor traps (e.g., dalantercept and sotatercept), and receptor kinase inhibitors (e.g., LY-2157299; ref. 46), whereas CD36 expression is increased by aspirin, dexamethasone, statins, and adalimumab (47–50). The effects of these drugs on MD remain to be investigated.

Disclosure of Potential Conflicts of Interest

No potential conflicts of interest were disclosed.

Authors' Contributions

Conception and design: R.A. DeFilippis, C. Fordyce, T.D. Tlsty
Development of methodology: R.A. DeFilippis, C. Fordyce, J. Zhao, T.D. Tlsty
Acquisition of data (provided animals, acquired and managed patients, provided facilities, etc.): J. Zhao, K. Kerlikowske
Analysis and interpretation of data (e.g., statistical analysis, biostatistics, computational analysis): R.A. DeFilippis, C. Fordyce, K. Patten, H. Chang, K. Kerlikowske, B. Parvin, T.D. Tlsty
Writing, review, and/or revision of the manuscript: R.A. DeFilippis, C. Fordyce, K. Kerlikowske, T.D. Tlsty
Administrative, technical, or material support (i.e., reporting or organizing data, constructing databases): C. Fordyce, J. Zhao, G.V. Fontenay, K. Kerlikowske, T.D. Tlsty
Study supervision: R.A. DeFilippis, T.D. Tlsty
Other (actually performed experiments): R.A. DeFilippis, K. Patten, C. Fordyce

Acknowledgments

The authors thank Dr. Blackburn (UCSF) for thoughtful discussions and advice, Tlsty laboratory members, particularly Dr. Gascard, for editorial assistance and the Nikon Imaging Center (UCSF) for imaging support. The authors also thank Dr. Au (UCSF), Drs. Hornik and Kim (Kaiser Foundation Research Institute, Oakland, CA), Dr. Sukumar (Johns Hopkins Sidney Kimmel Comprehensive Cancer Center, Baltimore, MD), and Ms. Wiles (Cooperative Human Tissue Network, Nashville, TN) for providing breast tissue samples.

Grant Support

This work was supported by NIH/NCI PO1 CA107584 to T.D. Tlsty, K. Kerlikowske, and B. Parvin (under LBNL contract No. DE-AC02-05CH11231), NIH/NCI RO1 CA097214 to T.D. Tlsty, CBCRP grant 14OB-0165 to T.D. Tlsty, NIH/NCI U54 CA143803 to T.D. Tlsty and B. Parvin (UC Riverside) and R01 Research Supplement for Underrepresented Minorities to C.A. Fordyce.

The costs of publication of this article were defrayed in part by the payment of page charges. This article must therefore be hereby marked *advertisement* in accordance with 18 U.S.C. Section 1734 solely to indicate this fact.

Received November 25, 2013; revised June 17, 2014; accepted July 9, 2014; published OnlineFirst August 29, 2014.

References

1. Tlsty TD, Coussens LM. Tumor stroma and regulation of cancer development. Annu Rev Pathol 2006;1:119–50.
2. Bing C, Trayhurn P. New insights into adipose tissue atrophy in cancer cachexia. Proc Nutr Soc 2009;68:385–92.
3. DeFilippis RA, Chang H, Dumont N, Rabban JT, Chen YY, Fontenay GV, et al. CD36 repression activates a multicellular stromal program shared by high mammographic density and tumor tissues. Cancer Discov 2012; 2:826–39.
4. Olumi AF, Grossfeld GD, Hayward SW, Carroll PR, Tlsty TD, Cunha GR. Carcinoma-associated fibroblasts direct tumor progression of initiated human prostatic epithelium. Cancer Res 1999;59:5002–11.
5. Barcellos-Hoff MH, Ravani SA. Irradiated mammary gland stroma promotes the expression of tumorigenic potential by unirradiated epithelial cells. Cancer Res 2000;60:1254–60.
6. McDaniel SM, Rumer KK, Biroc SL, Metz RP, Singh M, Porter W, et al. Remodeling of the mammary microenvironment after lactation promotes breast tumor cell metastasis. Am J Pathol 2006;168: 608–20.
7. Lyons TR, O'Brien J, Borges VF, Conklin MW, Keely PJ, Eliceiri KW, et al. Postpartum mammary gland involution drives progression of ductal carcinoma *in situ* through collagen and COX-2. Nat Med 2011;17:1109–15.
8. Finak G, Bertos N, Pepin F, Sadekova S, Souleimanova M, Zhao H, et al. Stromal gene expression predicts clinical outcome in breast cancer. Nat Med 2008;14:518–27.
9. Sharma M, Beck AH, Webster JA, Espinosa I, Montgomery K, Varma S, et al. Analysis of stromal signatures in the tumor microenvironment of ductal carcinoma *in situ*. Breast Cancer Res Treat 2010;123:397–404.
10. Guo YP, Martin LJ, Hanna W, Banerjee D, Miller N, Fishell E, et al. Growth factors and stromal matrix proteins associated with mammographic densities. Cancer Epidemiol Biomarkers Prev 2001;10:243–8.
11. Li T, Sun L, Miller N, Nicklee T, Woo J, Hulse-Smith L, et al. The association of measured breast tissue characteristics with mammographic density and other risk factors for breast cancer. Cancer Epidemiol Biomarkers Prev 2005;14:343–9.
12. Boyd NF, Byng JW, Jong RA, Fishell EK, Little LE, Miller AB, et al. Quantitative classification of mammographic densities and breast cancer risk: results from the Canadian National Breast Screening Study. J Natl Cancer Inst 1995;87:670–5.
13. Byrne C, Schairer C, Wolfe J, Parekh N, Salane M, Brinton LA, et al. Mammographic features and breast cancer risk: effects with time, age, and menopause status. J Natl Cancer Inst 1995;87:1622–9.
14. Silverstein RL, Febbraio M. CD36, a scavenger receptor involved in immunity, metabolism, angiogenesis, and behavior. Sci Signal 2009;2: re3.
15. Stone HB, Coleman CN, Anscher MS, McBride WH. Effects of radiation on normal tissue: consequences and mechanisms. Lancet Oncol 2003;4:529–36.
16. Mitchell JR, Wood E, Collins K. A telomerase component is defective in the human disease dyskeratosis congenita. Nature 1999;402:551–5.
17. Alder JK, Chen JJ, Lancaster L, Danoff S, Su SC, Cogan JD, et al. Short telomeres are a risk factor for idiopathic pulmonary fibrosis. Proc Natl Acad Sci U S A 2008;105:13051–6.
18. Wiemann SU, Satyanarayana A, Tsahuridu M, Tillmann HL, Zender L, Klempnauer J, et al. Hepatocyte telomere shortening and senescence are general markers of human liver cirrhosis. FASEB J 2002;16:935–42.

19. Fordyce C, Fessenden T, Pickering C, Jung J, Singla V, Berman H, et al. DNA damage drives an activin a-dependent induction of cyclooxygenase-2 in premalignant cells and lesions. Cancer Prev Res (Phila) 2010;3:190–201.
20. Fordyce CA, Patten KT, Fessenden TB, DeFilippis RA, Hwang ES, Zhao J, et al. Cell-extrinsic consequences of epithelial stress: activation of protumorigenic tissue phenotypes. Breast Cancer Res 2012;14: R155.
21. Holst CR, Nuovo GJ, Esteller M, Chew K, Baylin SB, Herman JG, et al. Methylation of p16(INK4a) promoters occurs *in vivo* in histologically normal human mammary epithelia. Cancer Res 2003;63:1596–601.
22. Romanov SR, Kozakiewicz BK, Holst CR, Stampfer MR, Haupt LM, Tlsty TD. Normal human mammary epithelial cells spontaneously escape senescence and acquire genomic changes. Nature 2001;409: 633–7.
23. Stampfer M, Hallowes RC, Hackett AJ. Growth of normal human mammary cells in culture. In Vitro 1980;16:415–25.
24. Treszezamsky AD, Kachnic LA, Feng Z, Zhang J, Tokadjian C, Powell SN. BRCA1- and BRCA2-deficient cells are sensitive to etoposide-induced DNA double-strand breaks via topoisomerase II. Cancer Res 2007;67:7078–81.
25. Lin KW, Yan J. The telomere length dynamic and methods of its assessment. J Cell Mol Med 2005;9:977–89.
26. Ismail IH, Wadhra TI, Hammarsten O. An optimized method for detecting gamma-H2AX in blood cells reveals a significant interindividual variation in the gamma-H2AX response among humans. Nucleic Acids Res 2007;35:e36.
27. Kataoka Y, Bindokas VP, Duggan RC, Murley JS, Grdina DJ. Flow cytometric analysis of phosphorylated histone H2AX following exposure to ionizing radiation in human microvascular endothelial cells. J Radiat Res 2006;47:245–57.
28. Branton MH, Kopp JB. TGF-β and fibrosis. Microbes Infect 1999;1: 1349–65.
29. Nagy L, Tontonoz P, Alvarez JG, Chen H, Evans RM. Oxidized LDL regulates macrophage gene expression through ligand activation of PPARγ. Cell 1998;93:229–40.
30. Harada K, Shintani Y, Sakamoto Y, Wakatsuki M, Shitsukawa K, Saito S. Serum immunoreactive activin A levels in normal subjects and patients with various diseases. J Clin Endocrinol Metab 1996;81: 2125–30.
31. Han J, Hajjar DP, Tauras JM, Feng J, Gotto AM Jr, Nicholson AC. Transforming growth factor-beta1 (TGF-β1) and TGF-β2 decrease expression of CD36, the type B scavenger receptor, through mitogen-activated protein kinase phosphorylation of peroxisome proliferator-activated receptor-gamma. J Biol Chem 2000;275:1241–6.
32. Chang H, DeFilippis RA, Tlsty TD, Parvin B. Graphical methods for quantifying macromolecules through bright field imaging. Bioinformatics 2009;25:1070–5.
33. Cirri P, Chiarugi P. Cancer associated fibroblasts: the dark side of the coin. Am J Cancer Res 2011;1:482–97.
34. Boyd NF, Dite GS, Stone J, Gunasekara A, English DR, McCredie MR, et al. Heritability of mammographic density, a risk factor for breast cancer. N Engl J Med 2002;347:886–94.
35. Broer L, Codd V, Nyholt DR, Deelen J, Mangino M, Willemsen G, et al. Meta-analysis of telomere length in 19 713 subjects reveals high heritability, stronger maternal inheritance and a paternal age effect. Eur J Hum Genet 2013;21:1163–8.
36. Epel ES, Blackburn EH, Lin J, Dhabhar FS, Adler NE, Morrow JD, et al. Accelerated telomere shortening in response to life stress. Proc Natl Acad Sci U S A 2004;101:17312–5.
37. Coppe JP, Desprez PY, Krtolica A, Campisi J. The senescence-associated secretory phenotype: the dark side of tumor suppression. Annu Rev Pathol 2010;5:99–118.
38. Fordyce CA, Heaphy CM, Bisoffi M, Wyaco JL, Joste NE, Mangalik A, et al. Telomere content correlates with stage and prognosis in breast cancer. Breast Cancer Res Treat 2006;99:193–202.
39. Willeit P, Willeit J, Mayr A, Weger S, Oberhollenzer F, Brandstatter A, et al. Telomere length and risk of incident cancer and cancer mortality. JAMA 2010;304:69–75.
40. Ursin G, Parisky YR, Pike MC, Spicer DV. Mammographic density changes during the menstrual cycle. Cancer Epidemiol Biomarkers Prev 2001;10:141–2.
41. Muttukrishna S, Fowler PA, George L, Groome NP, Knight PG. Changes in peripheral serum levels of total activin A during the human menstrual cycle and pregnancy. J Clin Endocrinol Metab 1996;81: 3328–34.
42. Checka CM, Chun JE, Schnabel FR, Lee J, Toth H. The relationship of mammographic density and age: implications for breast cancer screening. AJR Am J Roentgenol 2012;98:W292–5.
43. Ghosh K, Hartmann LC, Reynolds C, Visscher DW, Brandt KR, Vierkant RA, et al. Association between mammographic density and age-related lobular involution of the breast. J Clin Oncol 2010;28:2207–12.
44. Milanese TR, Hartmann LC, Sellers TA, Frost MH, Vierkant RA, Maloney SD, et al. Age-related lobular involution and risk of breast cancer. J Natl Cancer Inst 2006;98:1600–7.
45. Cuzick J, Warwick J, Pinney E, Duffy SW, Cawthorn S, Howell A, et al. Tamoxifen-induced reduction in mammographic density and breast cancer risk reduction: a nested case-control study. J Natl Cancer Inst 2011;103:744–52.
46. Fields SZ, Parshad S, Anne M, Raftopoulos H, Alexander MJ, Sherman ML, et al. Activin receptor antagonists for cancer-related anemia and bone disease. Expert Opin Investig Drugs 2013;22:87–101.
47. Vinals M, Bermudez I, Llaverias G, Alegret M, Sanchez RM, Vazquez-Carrera M, et al. Aspirin increases CD36, SR-BI, and ABCA1 expression in human THP-1 macrophages. Cardiovasc Res 2005;66:141–9.
48. Matasic R, Dietz AB, Vuk-Pavlovic S. Dexamethasone inhibits dendritic cell maturation by redirecting differentiation of a subset of cells. J Leukoc Biol 1999;66:909–14.
49. Ruiz-Velasco N, Dominguez A, Vega MA. Statins upregulate CD36 expression in human monocytes, an effect strengthened when combined with PPARγ ligands Putative contribution of Rho GTPases in statin-induced CD36 expression. Biochem Pharmacol 2004;67: 303–13.
50. Boyer JF, Balard P, Authier H, Faucon B, Bernad J, Mazieres B, et al. Tumor necrosis factor α and adalimumab differentially regulate CD36 expression in human monocytes. Arthritis Res Ther 2007;9:R22.